PCCP

Efficient Pourbaix diagrams of many-element compounds

Journal:	*Physical Chemistry Chemical Physics*
Manuscript ID	CP-ART-08-2019-004799.R1
Article Type:	Paper
Date Submitted by the Author:	28-Oct-2019
Complete List of Authors:	Patel, Anjli; Stanford University Nørskov, Jens; Technical University of Denmark, Chemical Engineering Persson, Kristin; Lawrence Berkeley Laboratory Montoya, Joseph; Toyota Research Institute

PCCP

ARTICLE TYPE

Cite this: DOI: 00.0000/xxxxxxxxxx

Efficient Pourbaix diagrams of many-element compounds

Anjli M. Patel,[a] Jens K. Nørskov,[b] Kristin Persson ,[c] and Joseph H. Montoya[d]

Received Date
Accepted Date

DOI: 00.0000/xxxxxxxxxx

Pourbaix diagrams have been used extensively to evaluate stability regions of materials subject to varying potential and pH conditions in aqueous environments. However, both recent advances in high-throughput material exploration and increasing complexity of materials of interest for electrochemical applications pose challenges for performing Pourbaix analysis on multidimensional systems. Specifically, current Pourbaix construction algorithms incur significant computational costs for systems consisting of four or more elemental components. Herein, we propose an alternative Pourbaix construction method that filters all potential combinations of species in a system to only those present on a compositional convex hull. By including axes representing the quantities of H^+ and e^- required to form a given phase, one can ensure every stable phase mixture is included in the Pourbaix diagram and reduce the computational time required to construct the resultant Pourbaix diagram by several orders of magnitude. This new Pourbaix algorithm has been incorporated into the pymatgen code and the Materials Project website, and it extends the ability to evaluate the Pourbaix stability of complex multicomponent systems.

1 Introduction

Pourbaix diagrams are an invaluable tool for exploring the corrosion profiles of materials as a function of ambient pH and electrochemical potential[1]. In recent years, high-throughput computational materials science efforts, like those from the Materials Project[2,3], have enabled more comprehensive Pourbaix diagrams to be constructed and disseminated from computational data[4,5]. These analyses have informed a number of computational studies of materials for electrochemical applications, aqueous electrocatalysis[6–9] and photoelectrocatalysis[10–12], non-equilibrium crystallization[13,14], and corrosion-resistant alloy design[15,16]. Pourbaix analysis of multicomponent systems is particularly valuable for finding elusive materials like acid-stable oxygen evolution catalysts[7], earth-abundant hydrogen evolution catalysts[17], and selective CO_2 reduction catalysts[18], which often require exploration in multi-element spaces. However, Pourbaix analysis has been limited to three or fewer elements, largely because computing the electrochemical phase stability of higher composition spaces has proven inefficient with existing methods.

In this report, we provide details of a modified method for Pourbaix diagram construction that enables diagrams to be constructed efficiently in much higher compositional spaces. This in turn enables phase stability analysis of similarly complex individual materials. We demonstrate this functionality with an analysis of the phase stability of a complex material for the alkaline oxygen evolution reaction (OER) and highlight our implementation in the open-source pymatgen[19] code and on the Materials Project website (materialsproject.org).

2 Pourbaix Algorithm

The primary bottleneck in pymatgen's prior implementation of multi-element Pourbaix diagrams resides in its pre-processing iteration over potential combinations of compounds. Based on the thermodynamic formalisms outlined in previous reports[4,20], this method iterates over all valid stoichiometric combinations of compounds in the chemical system that satisfy the compositional constraint particular to a given Pourbaix diagram (e.g. Fe:Cr = 2:1).

In this scheme, the scaling of Pourbaix diagram construction occurs with n choose m, where n is the number of compounds included and m is the number of elements included. Since larger numbers of elements tend to produce more entries on queries of the database, Pourbaix diagrams become prohibitively expensive after 3 elements. More explicitly, 4 or 5 element Pourbaix diagrams for the Ba-Sr-Co-Fe (present in $Ba_{0.5}Sr_{0.5}Co_{0.8}Fe_{0.2}O_{3-\delta}$ (BCSF)[21], an alkaline OER catalyst), and Al-Cu-Mn-Mg-Fe (present in some commercial Duralumin al-

[a] Department of Chemical Engineering, Stanford University, Stanford, CA, USA
[b] Department of Physics, Technical University of Denmark, Lyngby, Denmark
[c] Lawrence Berkeley National Laboratory and Department of Materials Science, University of California, Berkeley, CA
[d] Toyota Research Institute, 4440 El Camino Real, Los Altos, CA.; E-mail: joseph.montoya@tri.global

† Electronic Supplementary Information (ESI) available: [details of any supplementary information available should be included here]. See DOI: 10.1039/cXCP00000x/

‡ Additional footnotes to the title and authors can be included *e.g.* 'Present address:' or 'These authors contributed equally to this work' as above using the symbols: ‡, §, and ¶. Please place the appropriate symbol next to the author's name and include a `\footnotetext` entry in the the correct place in the list.

loys) would require $\sim 10^9$ and $\sim 10^{11}$ evaluations of selected combinations of compounds from the pool of materials, respectively.

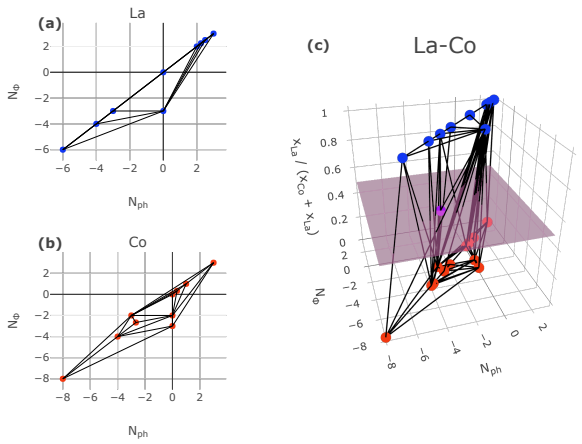

Fig. 1 Convex hull projections for La, Co, and La-Co chemical systems in $N_{pH} - N_\Phi$ and $N_{pH} - N_\Phi - x_{La}$ space. The highlighted plane in the figure corresponding to the La-Co system represents the composition constraint at a fixed non-OH composition, e.g. La:Co = 1:1 or $x_{La}/(x_{La}+x_{Co}) = 0.5$. Stable combinations of entries subject to this composition constraint may only be found in the simplices of the multi-dimensional convex hull which intersect this hyperplane. Note that in the 2-element case, mixed composition entries, such as the $LaCoO_3$ shown in purple, appear in the interior of the simplicial complex.

Considerable speedup is achieved by filtering for entries on the convex hull of the solid compositional phase diagram, which is at least partially motivated by physical reasoning that those materials should appear in the Pourbaix diagram absent any ions. This process, however, is complicated by the variable chemical potentials of H^+ and e^- on the Pourbaix diagram (but not on the compositional phase diagram) and the need to add ionic species, which still results in poor combinatoric scaling. The process was also further improved (e.g. in pymatgen) by virtue of it being easily parallelized, but this still only renders a factor of N speedup when much larger factors are required for the higher-element spaces to be tractable. In summary, with current hardware, execution times for 5-element and higher diagrams are estimated to be on the order of years.

To pre-filter the Pourbaix compounds that may appear on the hull, one can compute the convex hull in a similar manner as a pymatgen-implemented grand-canonical phase diagram, but in a space that includes fractional coefficients of electrons and protons. This essentially amounts to a grand-canonical phase diagram in $H^+ - e^- - H_2O - M_1 - M_2 - ... - M_n$, for which valid stable (i.e. minimal free energy of formation) compounds can be found by taking the convex hull in the space where μ_{H^+} and μ_{e^-} are treated as free variables (i.e. points corresponding to their reference energies are not include in the convex hull point inputs). For the purpose of finding stable combinations of entries, a 4-D convex hull and its corresponding simplicies in $N_{pH} - N_\Phi - x_1 - x_2 \ldots x_{n-1}$ space are sufficient, where N_{pH} and N_Φ are scaling factors for the Pourbaix energy[13] with respect to pH and applied potential, and x_n are non-OH fractions of the elemental composition. This hull and its corresponding simplices are illustrated for the La-Co Pourbaix system in Figure 1.

Under the assumption of ideal mixing, decomposition products in this space correspond to simplices on the convex hull, meaning that valid Pourbaix decomposition products can be limited to those which appear in a given simplex. The precise reduction in scaling will depend on the complexity of this hull, but it allows the combinatorial complexity to be isolated only to existing facets. In practice, this offers a reduction in the number of iterations by 2-3 orders of magnitude (see benchmarking in Figure 2).

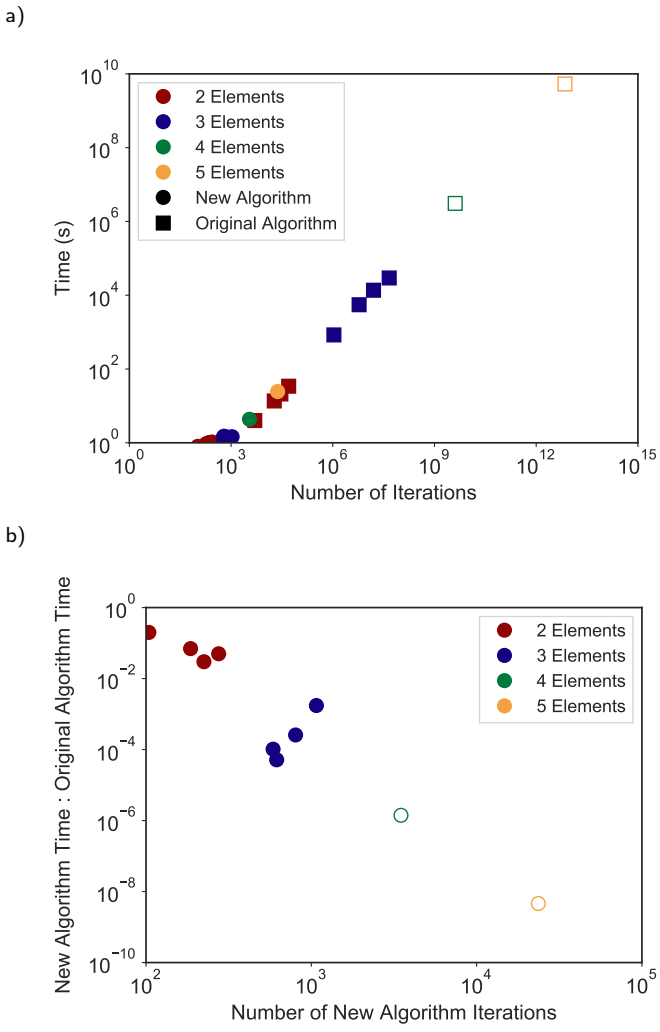

Fig. 2 a) CPU evaluation times and number of iterations required to analyze various multielement systems using the original and new Pourbaix algorithms. Hardware details are provided in supplementary information. Filled markers represent tested evaluation times, while unfilled markers represent extrapolated evaluation times based on the the average processing time from the 2 and 3-element performance runs. b) Ratio of new to original algorithm evaluation time as a function of number of iterations according to the new algorithm. These results suggest the new algorithm offers significant efficiency gains, especially for systems with many components.

We also note here that the determination of the Pourbaix regions in which the free energies of the corresponding species

is minimal are determined from a halfspace intersection of 2-dimensional planes corresponding to the pre-processed "multi-entry" phases (as termed in pymatgen), which differs from the grid-based methods implemented in ASE[22] and other reports[15]. However, our pre-processing might also be used to pre-filter compounds in a grid-based approach as these to reduce the iterative load at each evaluated point in E-pH space. We note also that grid-based approaches may still be necessary in more general phase-mapping cases, where the scaling of the free energies with state variables is not linearizeable or mixing is not ideal. This is because the ability to find halfspace intersections and the validity of the pre-processing convex hull filter depend on these assumptions.

Additional details on the thermodynamics and algorithm are provided in the supplementary information.

3 Benchmarking

To demonstrate the efficiency of this method, we benchmarked the Pourbaix diagram construction time for the compound with the highest number of elements in the Materials Project database ($Ba_2NaTi_2MnRe_2Si_8HO_{26}F$, mp-1215061), which completes in approximately 5 minutes via serial processing with no speedup by parallelization (computer hardware details provided in supplementary information). In contrast, the equivalent serial processing time for this system using the original Pourbaix construction algorithm in pymatgen is estimated to be on the order of $10^1 1$ years based averaged Pourbaix entry processing rates. This points to the added capability of featurizing the entire Materials Project dataset with Pourbaix decomposition grids, which can make Pourbaix diagrams more amenable to emerging data-intensive prediction methods like machine and deep learning. We include additional information related to algorithmic performance in the supplementary information.

To illustrate with another example, we include the heatmap corresponding to the decomposition energy against the Pourbaix diagram (using the methods developed by Singh et. al.[5]) of the perovskite $BaSrCo_7Fe_7O_{24}$ system, a model for the BSCF catalyst known for its high activity as an alkaline OER catalyst[21]. The Pourbaix diagram predicts that cation leaching is thermodynamically favorable with a modest driving force and that a passivation layer containing primarily Co, Fe, and possibly residual Sr should remain.

In Figure 3, we contrast the BCSF pourbaix diagram with that of the the $LaCoO_3$ system, which is predicted to be highly stable with very few favorable leaching processes in the oxygen evolution region. According to its Pourbaix diagram, $LaCoO_3$ has a large window of thermodynamic stability in the alkaline region of interest.

These predictions are consistent with detailed extended x-ray absorption fine structure (EXAFS) and high-resolution transmission electron microscopy (HRTEM) studies from Risch, May, and Shao-Horn et al., which reveal that A-site cation leaching is indeed present in x-ray diffraction-determined amorphous phases at the surface of BSCF. These phases form after extensive cycling but are not present in BSCF as-synthesized. Furthermore, their observation of the remarkable stability of $LaCoO_3$ as an OER catalyst via the same techniques is also predicted by our methodology[23,24].

To place this work in the appropriate context, we note that Pourbaix analysis may not tell the whole story of a given material's corrosion profile. Kinetics also play a significant role in corrosion, notably regarding the effects of various salt concentrations on electrolyte conductivity and consequently electrochemical rates.

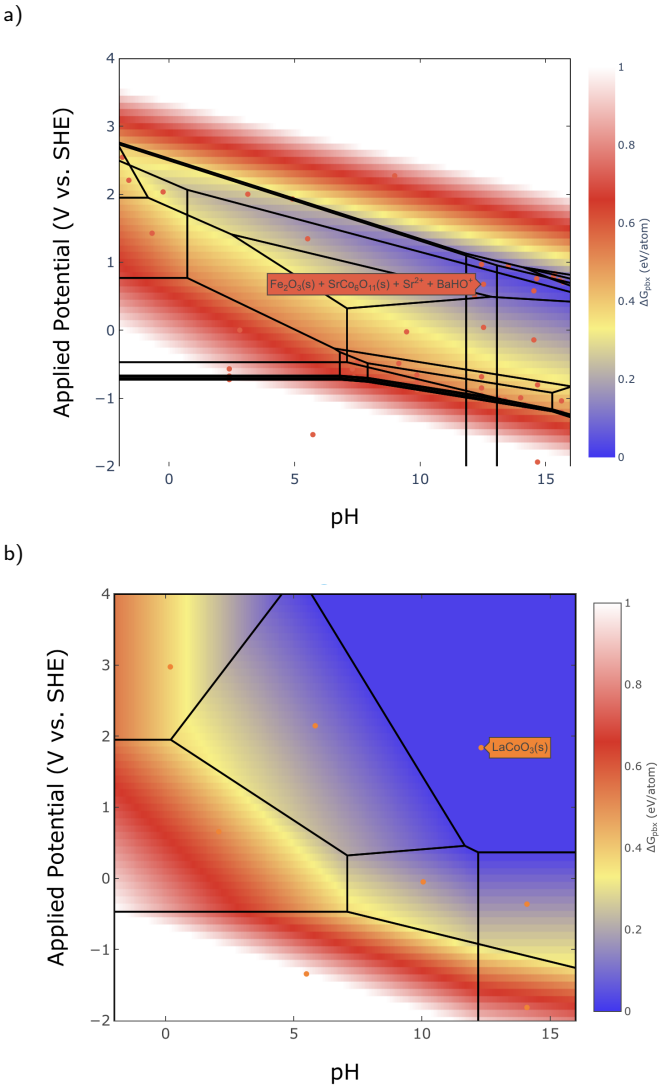

Fig. 3 Pourbaix stability diagrams for a) cubic perovskite $BaSrCo_7Fe_7O_{24}$ (mp-1075935), a model system for BSCF catalysts, and b) $LaCoO_3$. Decomposition energies in the alkaline OER region are within the metastability window (~0.1 eV/atom), and the stable phases include ion-phase Sr^{2+} and $BaHO^+$, indicating a modest driving force for cation leaching, whereas $LaCoO_3$ retains its surface structure after alkaline OER catalysis.[23,24]

Additionally, the stability of a given passivation layer will frequently depend on whether its inherent strain relative to the bulk material on which it forms is energetically tolerable. If not, as predicted by the Pilling-Bedworth ratio, passivation layers will frequently flake or crack. This represents a corrosion-based mode of material failure.[25,26] Furthermore, surface stabilities differ from

bulk stabilities, so the profile of nearest-surface region, which is often particularly relevant to a material's catalytic properties, may exhibit subtle differences from that of the bulk. These differences notably manifest in the role of Pourbaix-dependent surface coverage, which can influence reaction rates, particularly in alkaline OER [27–29].

Finally, we note that the quality of a given Pourbaix diagram will depend on the quality of the thermodynamic data which is used to generate it. In the cases presented here, all of the input data is from DFT-computed formation energies, which have well-known and systematically correctable errors [30]. This dependence is complicated by the fact that the formation energies of ions in the Materials Project scheme are computed relative to solids in order to allow for error cancellation between ionic and solid formation energies [4]. However, pymatgen's software infrastructure is agnostic to the source of a given solid formation energy, and experimental formation energies may be used alone or in concert with the computational data provided by the Materials Project application programming interface (API) [3].

4 Conclusions

In conclusion, we envision that this software functionality will have more general applications in the evaluation of corrosion resistance of complex alloys and of the stability of catalysts in high-throughput studies of water splitting and fuel cell reactions. As such, we have disseminated the implementation in the pymatgen.analysis.pourbaix_diagram module of the pymatgen open-source software, enabling its use on the Materials Project website. Ultimately, it is our hope that efficient Pourbaix analysis of these complex compounds will enable new insights to be derived on materials which were previously intractable to analyze.

Conflicts of interest

There are no conflicts to declare.

Acknowledgements

The authors acknowledge the Toyota Research Institute (TRI) and the Accelerated Materials Design and Discovery (AMDD) program for support through the SUNCAT Center for Interface Science and Catalysis and the National Science Foundation Graduate Research Fellowship Program (NSF GRFP).

Notes and references

1 M. Pourbaix, *Corrosion Science*, 1974, **14**, 25–82.

2 A. Jain, S. P. Ong, G. Hautier, W. Chen, W. D. Richards, S. Dacek, S. Cholia, D. Gunter, D. Skinner, G. Ceder and K. A. Persson, *Commentary: The materials project: A materials genome approach to accelerating materials innovation*, 2013.

3 S. P. Ong, S. Cholia, A. Jain, M. Brafman, D. Gunter, G. Ceder and K. A. Persson, *Computational Materials Science*, 2015, **97**, 209–215.

4 K. A. Persson, B. Waldwick, P. Lazic and G. Ceder, *Physical Review B*, 2012, **85**, 235438.

5 A. K. Singh, L. Zhou, A. Shinde, S. K. Suram, J. H. Montoya, D. Winston, J. M. Gregoire and K. A. Persson, *Chemistry of Materials*, 2017, **29**, 10159–10167.

6 J. Rossmeisl, J. Greeley and G. S. Karlberg, *Fuel Cell Catalysis: A Surface Science Approach*, 2008, pp. 57–92.

7 L. Zhou, A. Shinde, J. H. Montoya, A. Singh, S. Gul, J. Yano, Y. Ye, E. J. Crumlin, M. H. Richter, J. K. Cooper, H. S. Stein, J. A. Haber, K. A. Persson and J. M. Gregoire, *ACS Catalysis*, 2018, **8**, 10938–10948.

8 A. Marjolin and J. A. Keith, *ACS Catalysis*, 2015, **5**, 1123–1130.

9 B. Han, M. Risch, S. Belden, S. Lee, D. Bayer, E. Mutoro and Y. Shao-Horn, *Journal of the Electrochemical Society*, 2018, **165**, F813–F820.

10 A. K. Singh, J. H. Montoya, J. M. Gregoire and K. A. Persson, *Nature Communications*, 2019, **10**, 443.

11 I. E. Castelli, F. Hüser, M. Pandey, H. Li, K. S. Thygesen, B. Seger, A. Jain, K. A. Persson, G. Ceder and K. W. Jacobsen, *Advanced Energy Materials*, 2015, **5**, 1400915.

12 Q. Yan, G. Li, P. F. Newhouse, J. Yu, K. A. Persson, J. M. Gregoire and J. B. Neaton, *Advanced Energy Materials*, 2015, **5**, 1401840.

13 W. Sun, D. A. Kitchaev, D. Kramer and G. Ceder, *Nature Communications*, 2019, **10**, 573.

14 L. A. Wills, X. Qu, I.-Y. Chang, T. J. L. Mustard, D. A. Keszler, K. A. Persson and P. H.-Y. Cheong, *Nature Communications*, 2017, **8**, 15852.

15 R. Ding, J. X. Shang, F. H. Wang and Y. Chen, *Computational Materials Science*, 2018, **143**, 431–438.

16 L.-F. Huang, J. R. Scully and J. M. Rondinelli, *Annual Review of Materials Research*, 2019, **49**, 53–77.

17 B. Hinnemann, P. G. Moses, J. Bonde, K. P. Jørgensen, J. H. Nielsen, S. Horch, I. Chorkendorff and J. K. Nørskov, *Journal of the American Chemical Society*, 2005, **127**, 5308–5309.

18 D. A. Torelli, S. A. Francis, J. C. Crompton, A. Javier, J. R. Thompson, B. S. Brunschwig, M. P. Soriaga and N. S. Lewis, *ACS Catalysis*, 2016, **6**, 2100–2104.

19 S. P. Ong, W. D. Richards, A. Jain, G. Hautier, M. Kocher, S. Cholia, D. Gunter, V. L. Chevrier, K. A. Persson and G. Ceder, *Computational Materials Science*, 2013, **68**, 314–319.

20 W. T. Thompson, M. H. Kaye, C. W. Bale and A. D. Pelton, *Uhlig's Corrosion Handbook: Third Edition*, 2011, pp. 103–109.

21 J. Suntivich, K. J. May, H. A. Gasteiger, J. B. Goodenough and Y. Shao-Horn, *Science*, 2011, **334**, 1383–1385.

22 A. Hjorth Larsen, J. Jørgen Mortensen, J. Blomqvist, I. E. Castelli, R. Christensen, M. Dułak, J. Friis, M. N. Groves, B. Hammer, C. Hargus, E. D. Hermes, P. C. Jennings, P. Bjerre Jensen, J. Kermode, J. R. Kitchin, E. Leonhard Kolsbjerg, J. Kubal, K. Kaasbjerg, S. Lysgaard, J. Bergmann Maronsson, T. Maxson, T. Olsen, L. Pastewka, A. Peterson, C. Rostgaard, J. Schiøtz, O. Schütt, M. Strange, K. S. Thygesen, T. Vegge, L. Vilhelmsen, M. Walter, Z. Zeng and K. W. Jacobsen, *Journal of Physics: Condensed Matter*, 2017, **29**, 273002.

23 M. Risch, A. Grimaud, K. J. May, K. A. Stoerzinger, T. J. Chen, A. N. Mansour and Y. Shao-Horn, *Journal of Physical Chemistry C*, 2013, **117**, 8628–8635.

24 K. J. May, C. E. Carlton, K. A. Stoerzinger, M. Risch, J. Suntivich, Y. L. Lee, A. Grimaud and Y. Shao-Horn, *Journal of Physical Chemistry Letters*, 2012, **3**, 3264–3270.

25 A. T. Fromhold, *Theory of Metal Oxidation*, 1976, 1–16.

26 X. Zhou, G. E. Thompson, P. Skeldon, G. C. Wood, K. Shimizu and H. Habazaki, *Corrosion Science*, 1999, **41**, 1599–1613.

27 Y. L. Lee, M. J. Gadre, Y. Shao-Horn and D. Morgan, *Physical Chemistry Chemical Physics*, 2015, **17**, 21643–21663.

28 H. A. Hansen, J. Rossmeisl and J. K. Nørskov, *Physical Chemistry Chemical Physics*, 2008, **10**, 3722–3730.

29 Z. W. Ulissi, A. R. Singh, C. Tsai and J. K. Nørskov, *Journal of Physical Chemistry Letters*, 2016, **7**, 3931–3935.

30 A. Jain, G. Hautier, S. P. Ong, C. J. Moore, C. C. Fischer, K. A. Persson and G. Ceder, *Physical Review B*, 2011, **84**, 045115.